

---

Original Paper

---

# CFD and surrogates-based inducer optimization

Tomáš Krátký<sup>1</sup>, Lukáš Zavadil<sup>1</sup> and Vít Doubrava<sup>2</sup>

<sup>1</sup>Centre of Hydraulic Research

Jana Sigmunda 190, Lutín, 783 49, Czech Republic, t.kratky@sigma.cz, l.zavadil@sigma.cz

<sup>2</sup>SIGMA Research and Development Institute

Jana Sigmunda 79, Lutín, 783 49, Czech Republic, v.doubrava@sigma.cz

## Abstract

Due to the nature of cavitation numerical analyses, computational optimization of a pump with respect to the cavitation properties is extremely demanding. In this paper it is shown how a combination of Transient Blade Row (TBR) method and some simplifications can be used for making the optimization process more efficient and thus possible on current generation of hardware. The aim of the paper is not the theory of hydraulic design. Instead, the practical aspects of numerical optimization are shown. This is done on an example of a radial pump and a combination of ANSYS CFX, ANSYS software tools and custom scripts is used. First, a comparison of TBR and fully-transient simulation is made. Based on the results, the TBR method is chosen and a parametric model assembled. Design of Experiment (DOE) table is computed and the results are used for sensitivity analysis. As the last step, the final design is created and computed as fully-transient. In conclusion, the results are discussed.

**Keywords:** Design Optimization, CFD, Cavitation, Inducer, TBR, ANSYS CFX.

## 1. Introduction

Cavitation properties of pump are one of the major parameters for judging the pump performance. Thus improving these properties is an important part of a hydraulic development. Unfortunately, obtaining a NPSH<sub>3</sub> curve requires computing multiple head drop curves. Due to high sensitivity of CFD algorithms to pressure drops, computing a head drop curve requires multiple CFD analyses, gradually lowering suction heads.

This makes CFD-aided optimizations of a pump with respect to the cavitation properties very difficult and taxing. Yet still, in some cases, a TBR method can be (with certain limits) employed to our advantage. This is especially true for an inducer, a common way of improving NPSH<sub>3</sub> characteristic. For the purposes of CFD hydraulic design, inducer has two aspects:

1. Its influence on pump hydraulic performance remains very similar through wide variety of shapes. This allows focusing on cavitation performance during the design phase.
2. It is axisymmetric. This means TBR method can be employed for numerical analyses, resulting in a great reduction of computational costs. Although this method only gives accurate results in a vicinity of optimal flow rates, it is still valuable for great part of the design process.

Due to this, optimizing an inducer is relatively viable. In the next part, such a CFD-aided optimization of an inducer will be demonstrated on a specific pump. Due to time-proven results, great meshing tools and scripting abilities, ANSYS CFX was chosen for this task.

## 2. The pump

### 2.1 The original pump

The pump is radial with horizontally mounted shaft and spiral casing; shrouded impeller has six blades. The pump has the dimensionless specific speed [10]  $\omega_s \cong 0.48$ , with outlet-diameter of the impeller  $D = 360\text{mm}$ . The performance characteristics were measured in an experiment in hydraulic laboratory. To enhance the pump's potential, lowering its NPSH<sub>3</sub> characteristic for flow rates in the working range was necessary. The most suitable solution was adding an inducer upstream of the impeller.

## 2.2 The inducer

The hydraulic design was based on [10]. The inducer has three blades, and it was designed for 110% of QOPT. Two variants were developed, the second one performing better for the given application, especially in the sub-optimal flow rates.

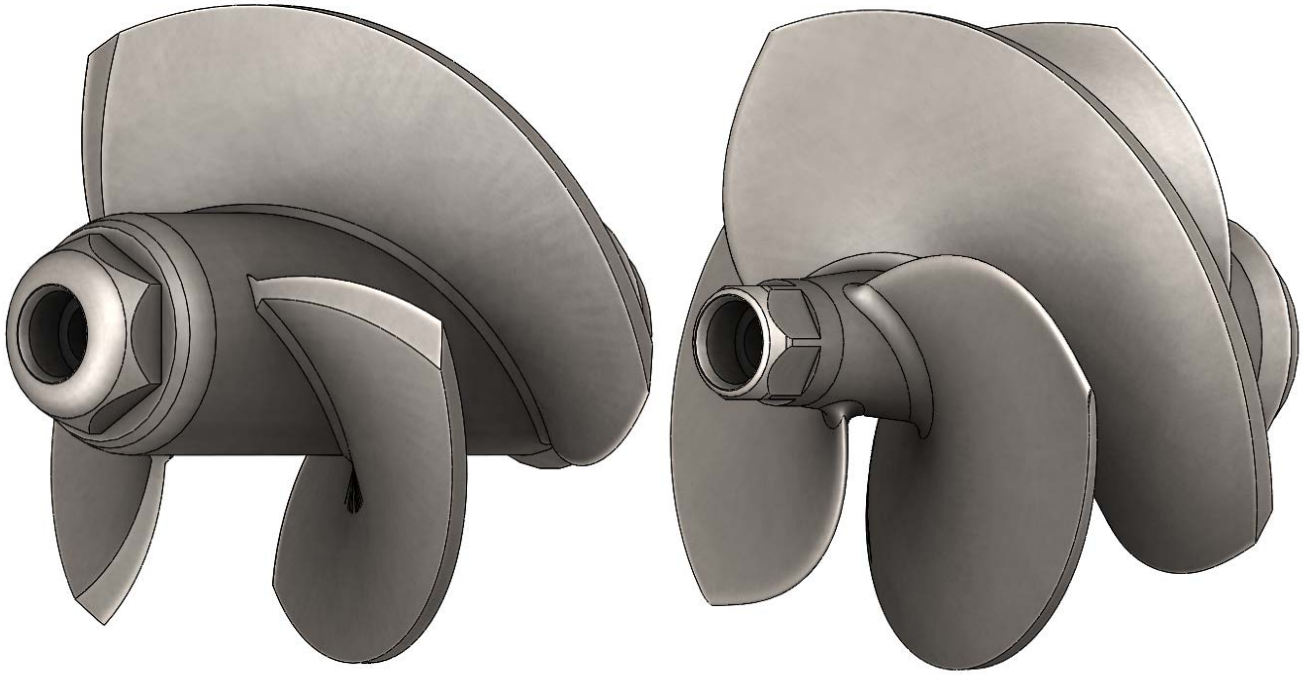


**Fig. 1** First (left) and second (right) variant of the inducer.

## 2.3 Numerical analysis of the pump performance

Using ANSYS CFX software tools, a fully-transient cavitation analysis on the complete geometry was performed. The mesh was mostly hexahedral, with tetra/prism for the volute. The resultant mesh had about 1 million of nodes. Straight sections were added to the inlet and the outlet. Based on empiric experiences, the added length was selected as 5 diameters at the inflow and 8 diameters at the outflow. These minimize chance of backflows on the boundaries. The result is better convergence and numerical stability. The impeller and inducer areas were rotating, with rotor – stator interfaces on the boundaries.

As a turbulence model, the SST  $k-\omega$  model offered by ANSYS CFX was used. It is the most suitable model for pumps, because it combines high efficiency with high accuracy of describing near-wall flows. Homogenous model was used for the multiphase flow (with water and water vapour as the fluids), and Rayleigh Plesset for cavitation. The boundary conditions were standard for cavitation analysis – pressure head at the inlet and mass flow rate at the outlet. The pump head was evaluated as a pressure difference between the inlet and the outlet.

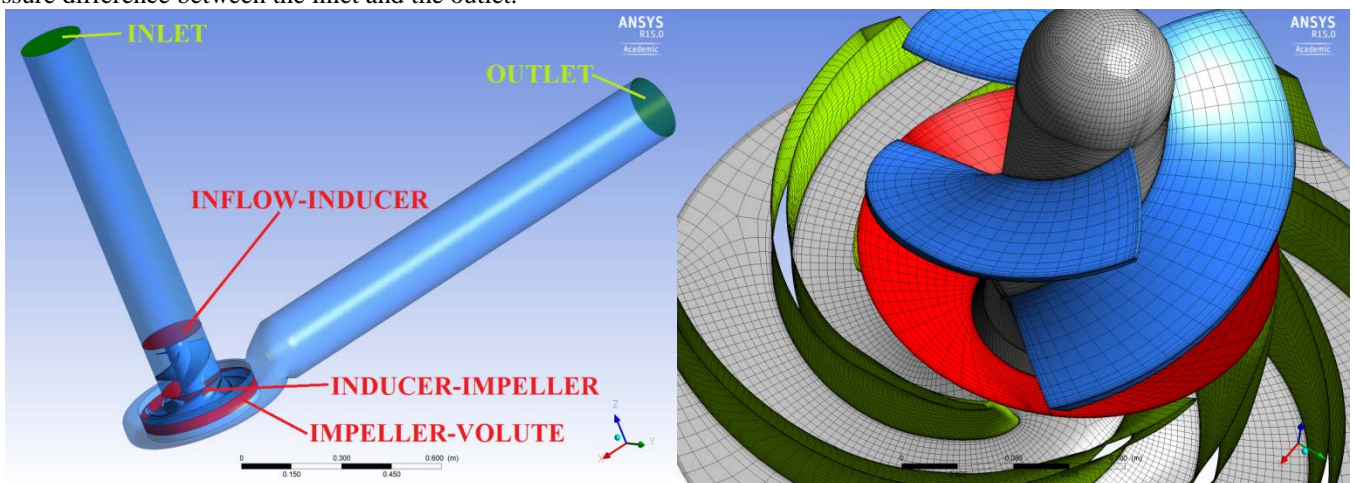


**Fig. 2** The assembled fully-transient model and mesh details. Interfaces are in red.

Not only is the multiphase CFD analysis more resources consuming than a single phase one. On top of that, the CFD codes are inherently sensitive to pressure changes during cavitation analyses. When such a change occurs, numerical violation of continuity equation often results in “spikes” of below the vapour pressure in some locations. This is not a problem for single-phase flow and these “spikes” disappear in a few iterations. But for cavitation analysis, below the vapour pressure equals cavitation cavern creation. And for low suction pressure, such a cavern grows rapidly once it is created. As a result, too steep inlet pressure drop during the analysis can cause early (and artificial) breakdown and skew the results.

Due to this phenomenon, NPSH3 computation is very taxing, since for each point on the NPSH3 characteristic, the head drop curve needs to be computed. First for a high enough suction pressure, to obtain a head value not hindered by cavitation effects, and then with gradually lower and lower pressure, up to a point where 3% head drop occurs. The proven method is lowering the

pressure in smaller steps – the closer to the expected point of drop, the smaller drops and higher iterations count, to counter worsened numerical stability once the cavitation effects come into play.

Head drop curve example

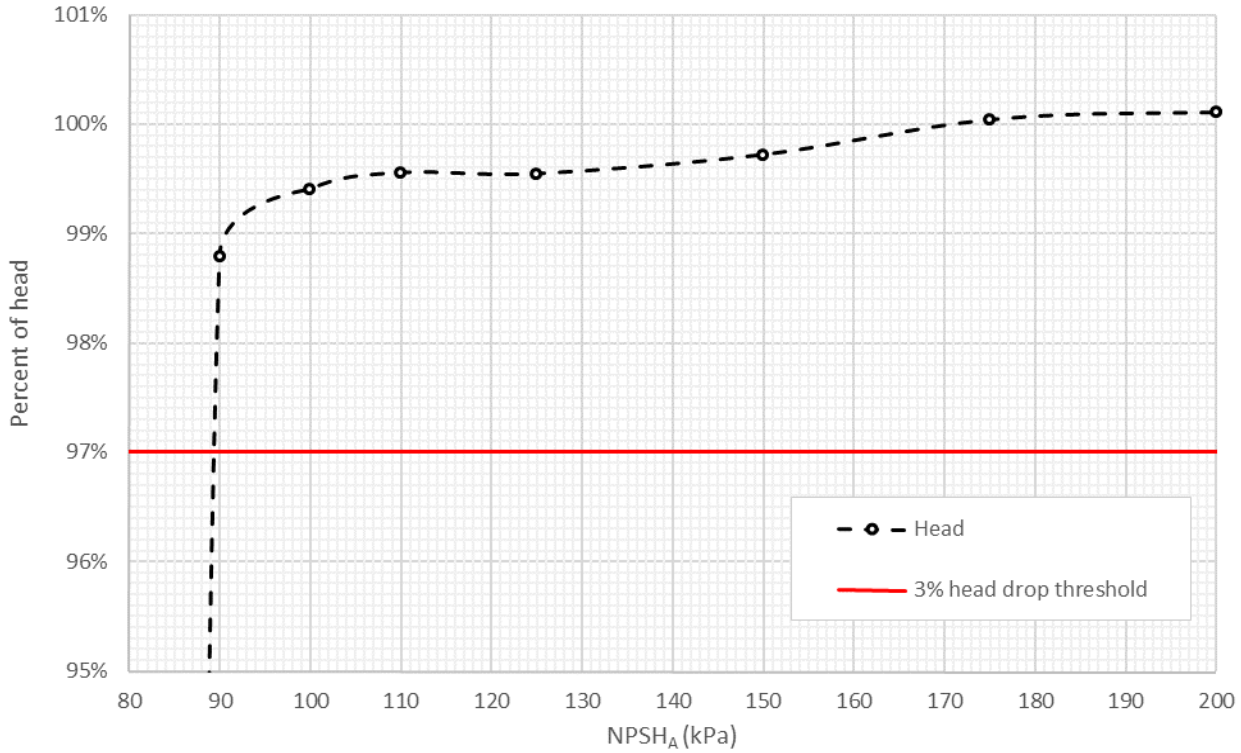


Fig. 3 And example of a head drop curve and NPSH<sub>3</sub> evaluation

NPSH<sub>3</sub> characteristics

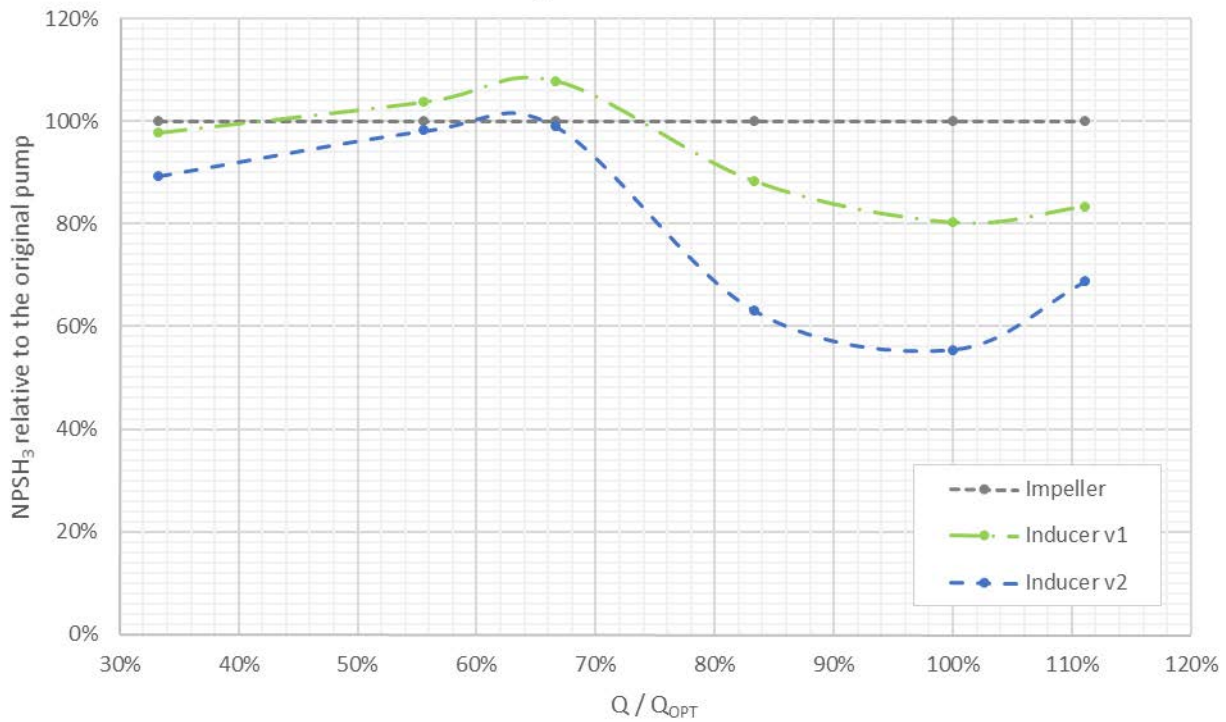


Fig. 4 Comparison of NPSH<sub>3</sub> characteristics of the pump with and without the inducers.

### 3. Numerical optimization

#### 3.1 Optimization and sensitivity analysis

Due to the very nature of CFD computations, traditional optimization algorithms do not yield great results within reasonable number of iterations. The numbers obtained by CFD tend to “fluctuate” a bit, i.e. two computations of the same design can give slightly different results for many different reasons, such as the mesh used, number of iterations during the simulation and rounding errors. The differences are not significant enough to skew design performance evaluation. But optimization algorithms

based on direction searching have hard times to deal with these errors. To counter these problems, another approach is currently widely used for CFD-aided optimization - the so-called Response Surface Method (RSM) [1].

This procedure uses statistical approach. For given parameters, samples for the Design of Experiment (DOE) table are generated. Then the samples are computed and, based on the results and selected objective function, sensitivity analysis is performed. For each parameter, sensitivity (how much it influences the objective function) is estimated. This way it is much easier to filter wrong results (if there are any) and deal with the CFD inherent slight inaccuracy. It also allows for much easier parallelism, because each sample can be computed independently. With a well-defined parametric model and sufficient number of samples, it is possible to get sufficient sensitivity estimates [9]. Usually, full number of parameters is chosen for the first sensitivity analysis. Then, based on the results, only the most important ones are used, parameter ranges are updated and another DOE is generated and computed. And sensitivity is assessed more accurately with the new data.

Two sensitivity analyses are usually sufficient for estimating the “best” design and verify it numerically. If the results are not satisfying, either a suitable optimization algorithm can be used from this point on, or repeat the process with different set of parameters / ranges.

### 3.2 The approach to the optimization

As described above, computing one point on NPSH<sub>3</sub> curve usually requires one stationary and 10 to 15 fully-transient (and multiphase) runs. When compared to one stationary and one transient ones needed for one point on the characteristic curve, we are talking about 20 times the computational time. This renders a numerical optimization of a pump with respect to the cavitation properties virtually impossible on anything but a very powerful hardware with (at least) hundreds of cores.

This is true when considering the “proper” way of computing NPSH<sub>3</sub>. But, for the demands of the optimization, we can make some simplifications without sacrificing too much. First, it is convenient to lower the suction pressure gradually during one computation. Normally, this is not used, because it is too risky (and we also usually want the head drop curve shape). We do not know exactly, where the breakdown occurs, and too low final pressure value means a wasted analysis. For DOE samples it is a worthy trade-off, though. We might not know exactly where the head drop occurs, but we know the target – we want an improvement of the initial design.

The solution is starting from a very high suction pressure (to ensure a proper transition from the initial file with different geometry) and lowering it to a point just a small bit above the NPSH<sub>3</sub> of the original design. With the right tweaking, we can avoid the artificial breakdown in most cases. Using this approach, we get sensible results for the good variants and the rest can be easily penalized by the objective function. Due to the statistical nature of the sensitivity analysis, using these results in not a big problem. In case we need to differentiate the samples a bit more, we can than easily compute the selected ones for even lower pressure(s). And in exchange for these trade-offs we now need only between one and two analyses per NPSH<sub>3</sub> point for each variant, instead of 10 to 15.

To further leverage this advantage and reduce computational costs even more, another simplification can be employed - the so-called Transient Blade Row (TBR) method.

### 3.3 TBR method and its limitations

For axisymmetric geometries and in a vicinity of an optimal flow rate, TBR model allows for accurate computations of rotor and stator blades interactions. But instead of the full geometry, only the minimal number of blade passages to match the different numbers in inducer and impeller are required. Volute is not axisymmetric, but since the cavitation appears first in the inducer and advances further to the impeller as the suction pressure goes down, there’s basically no cavitation in volute up to the point of breakdown. Replacing the volute by an axisymmetric confusor gives different absolute head numbers, but keeps the head drop curve shape very close to the original. Experiences show a TBR model with described necessary modifications gives sufficiently accurate results in a vicinity of optimal flow rate.

In our case, the TBR model includes one inducer passage and two impeller ones. For better convergence and numerical stability, a straight section was added to the inlet and confusor replacement of the volute was added to the outlet. The resulting assembled model had about 250 thousands of nodes and thanks to the volute replacement, the mesh could be fully structured.

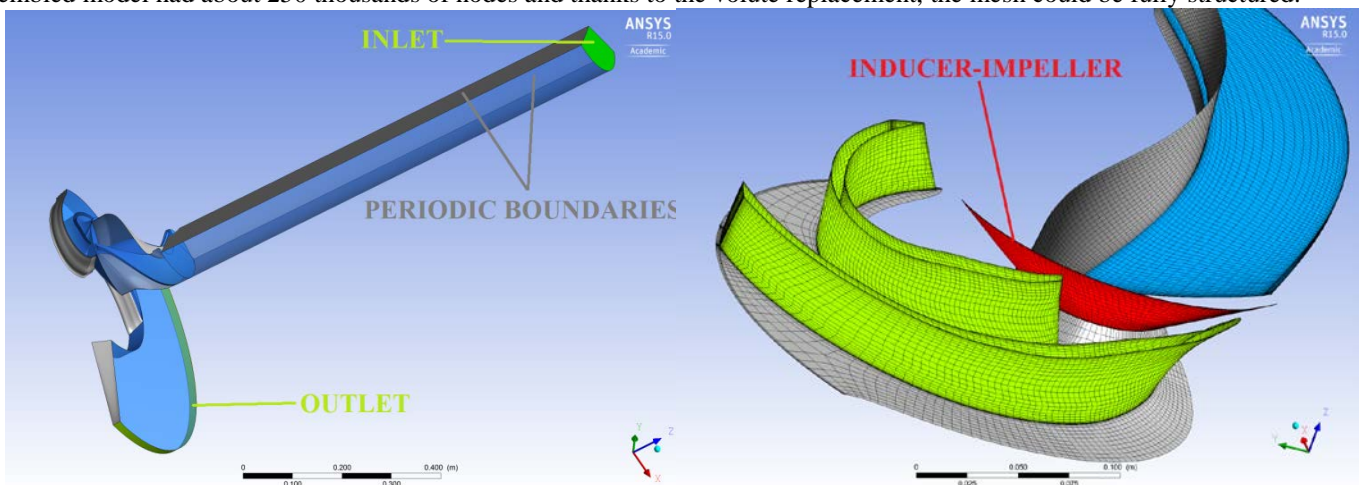


**Fig. 5** The TBR model and mesh details. Interfaces are in red.

Compared to the fully-transient model this equals to more than four times faster computations. For 50%, 100% and 120% of optimal flow rate the combination of the TBR model and the aforementioned slow pressure drop during the computation was used.

The results were compared to the original ones.

**Table 1** Fully-transient and TBR model NPSH<sub>3</sub> computation comparison

50% Q <sub>OPT</sub>			100% Q <sub>OPT</sub>			120% Q <sub>OPT</sub>		
Pressure (kPa)	H [m]		Pressure (kPa)	H [m]		Pressure (kPa)	H [m]	
	full	TBR		full	TBR		full	TBR
1000	183,1	187,1	1000	154,1	155,5	1000	128,4	137,1
55	182,2	187,8	45	152,6	152,9	125	127,2	136,4
52	break.	188,6	40	break.	break.	110	break.	break.

As expected, 100 a 120% results are very close (*break* means *cavitation breakdown*). As a bonus, TBR generally displays faster convergence and better stability, mostly due to the lower frequencies absence. These traits make it ideal for computing the DOE samples, especially when combined with the progressive pressure change during one computation.

### 3.4 Parametric model of the inducer

For the purposes of testing the optimization procedures, the second variant was chosen as initial design. The parametric model was done using ANSYS DesignModeler and based on the usual pump hydraulic design standards [1, 2, 10]. I.e. hub and shroud meridional shapes, leading edge (LE) and trailing edge (TE) position and shape, beta angles distribution and blade thickness. The blade was defined by three curves – on the hub, on the shroud, and the midspan. Based on the thickness, the actual blade is then created around these curves.

The parametric model proved to be a major challenge. As is shown in a literature [10], using the so-called sweep-back for the LE has positive effect on the inducer performance. The values between 65 and 90 degrees are considered to be optimal. Unfortunately, LE and TE beta angles are relatively strictly given. For LE, beta should be slightly above the shockless entry angle, computed for the highest flow from the working range. Lower betas lead to cavitation on the pressure side of the blade, resulting in sharp increase in NPSH<sub>3</sub>. Higher betas, on the other hand, are “safer” for higher flow rates, but limit inducer performance in lower end of the working range. On top of that, holding the LE beta angle for a portion of the blade shows as desirable, too. Value around 20% is recommended [10].

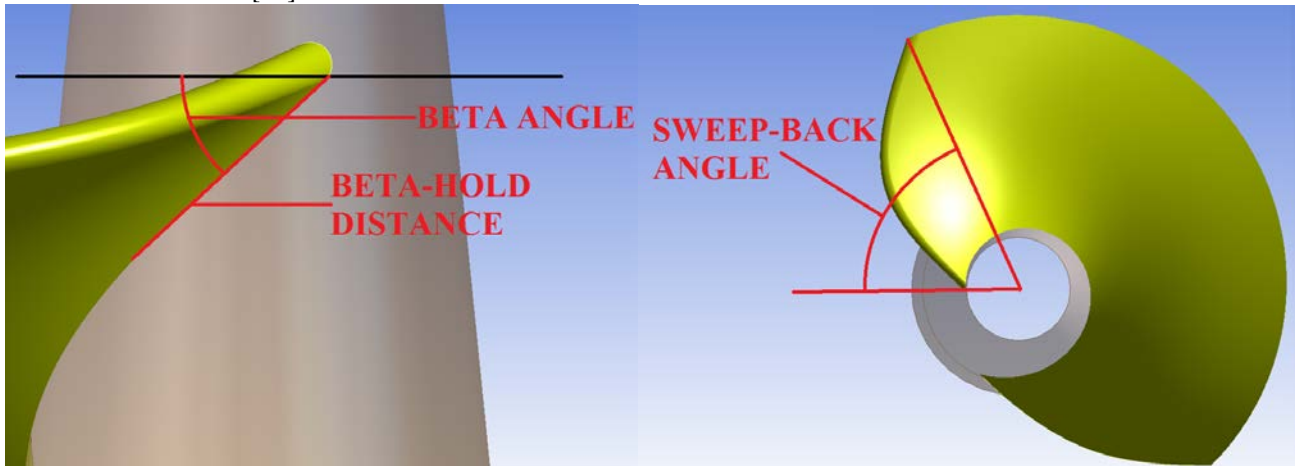


**Fig. 6** Beta and sweep-back angles illustration

As a result of these opposing requirements, avoiding waved blade is difficult, especially for higher sweep-back values. Also, since the blades were defined by three curves, preventing “waving” the blade in radial direction can be tricky. When modelling the geometry manually, these are not big problems, as you can always “fine-tune” it visually. For generating DOE samples, this is not possible. ANSYS DesignModeler and BladeModeler were used for the parametric model creation. Since there was no tool for an automatic blade shape smoothing, custom scripts were necessary. For each variant, the feasible beta distribution was generated using Microsoft Excel and Visual Basic for Applications (VBA).

In total, there were 20 parameters: LE and TE beta angles, portion of the blade with the same beta as on LE, LE eccentricity and blade thickness. The parameters were prescribed on the hub and the shroud. Midspan data were averaged from the hub and the shroud, skewed to one of these by a parameter. To avoid a necessity of re-computing inflow and impeller meshes, the inlet and outlet interfaces remained fixed for all variants. For automatic meshing, ANSYS TurboGrid was an ideal candidate. It was able to create structured meshes for most of the samples, fast and with good quality.

### 3.5 Assembling and computing the DOE table

A combination of ANSYS DesignXplorer, WorkBench (WB) and Excel was used. Design of Experiment (DOE) table generated by DesignXplorer was exported to Excel, and for each sample, a WB script was generated. Then the CFX solver input files were created by calling WB in batch mode. This way it was much easier to control the process and deal with geometry and mesh generation errors. To get a good estimation of the objective function dependency on parameters, a DOE table with around 120 samples (denoted by DOE 1) was created.

Computations were run on HPC cluster, launching scripts again created by Excel VBA. For all the samples, the same initial file from the original inducer was used. This is one the major advantages of the sensitivity analysis approach – each of the DOE

sample computation is independent on the other ones. As a result of this advantage, the performance scales linearly with the number of simultaneously running simulations. Due to the hardware and CFD limitations, this cannot be achieved with standard optimization by increasing number of cores, at least not for 1 million nodes simulation.

### 3.6 Sensitivity analysis and results evaluation

The simulations data were exported to Excel and evaluated. Head was averaged on last two periods. As other criteria, vapour volume in the inducer and impeller were calculated by a CFD-Post script. Based on these numbers, the objective function was calculated for each sample and imported back to the DOE table in DesignXplorer. The objective function values were higher for better variants. Using these data, the sensitivity analysis was performed.

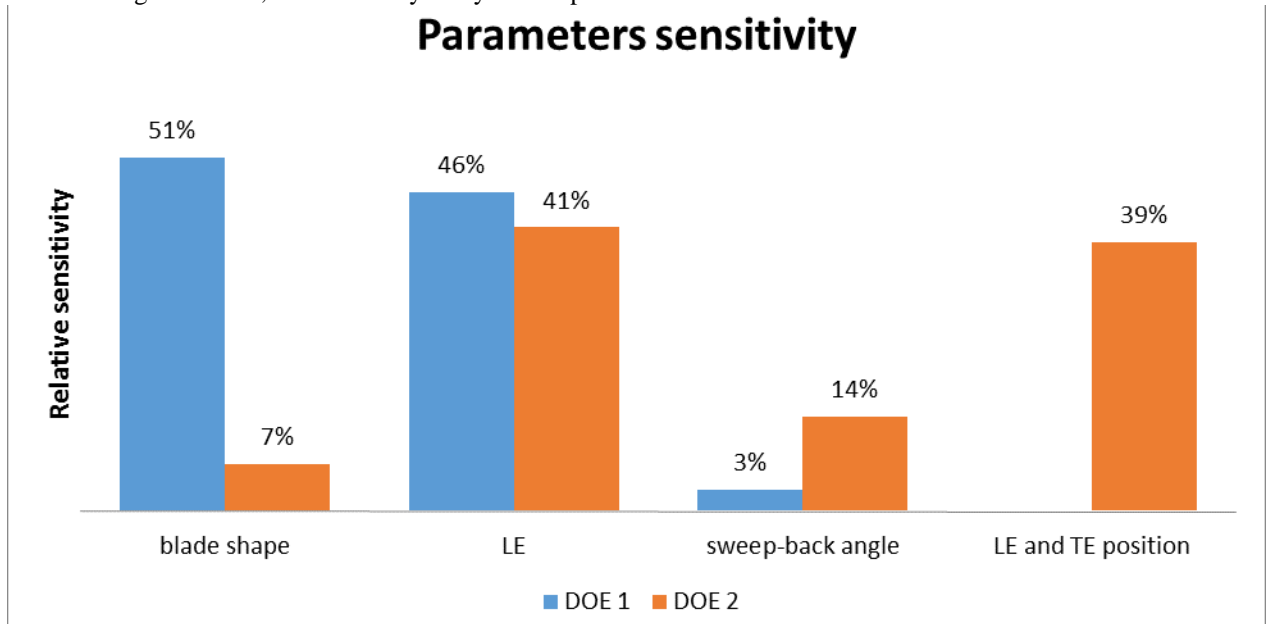


**Fig.** Results of the sensitivity analysis for selected parameters. For better clarity, the parameters are divided into categories.

Blade shape (beta angle and thickness distribution) and LE shape and angle were the most influential parameters. Surprisingly, the sweep-back angle only played a minor role, quite the opposite of our expectations based on [10] and the original inducer design. It was probably due to the fact that increasing the sweep-back angle narrows the possibilities of good beta angle distribution. This “waved blade” problem adds error to the model and skews the results, especially for the wide range of parameters in the first DOE. Still, for most of the parameters, optimal values could be estimated. The “optimum” decided with the first DOE was used as the centre of the new area for sensitivity analysis.

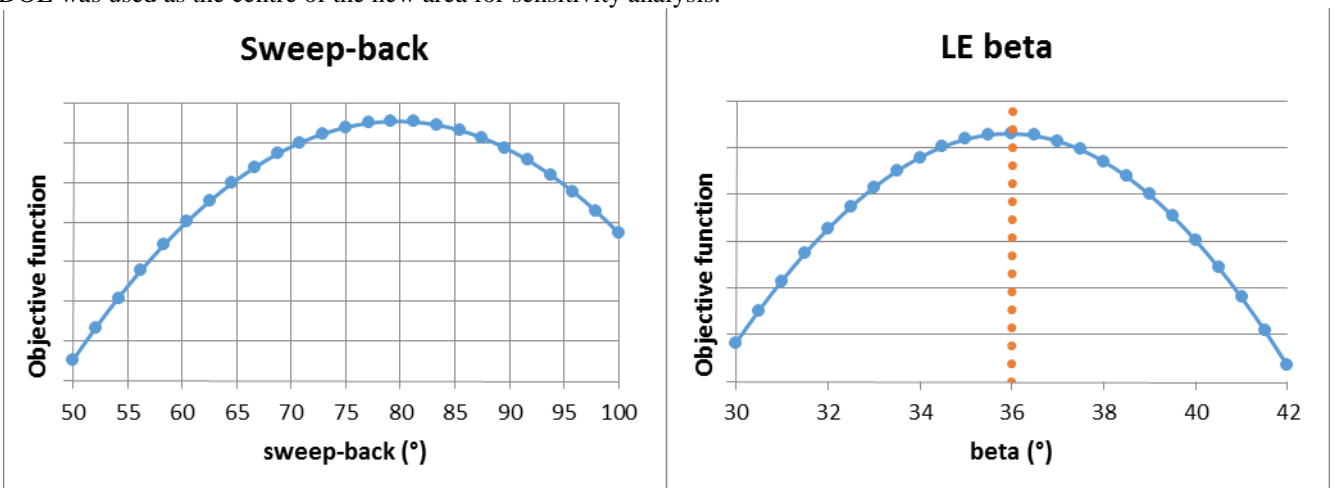


**Fig. 8** Objective function for sweep-back and LE beta angles. Red dashed line denotes a theoretical beta optimum.

As the next step, the reduced model was assembled, with narrower parameter ranges. There were 9 monitored parameters: Four parameters were added for LE and TE meridional positions, and the most important beta angles and sweep-back angle parameters remained. For the lower number of parameters, another DOE (denoted as DOE 2) containing 50 samples was created. Employing the same scripts as in the previous case, the solver files were generated and computed on the HPC cluster.

Lower number of samples allowed for computing two inlet pressures instead of one. Thanks to this, the NPSH<sub>3</sub> could be assessed more accurately. Once again, the vapour volumes were computed and included in the objective function values. Based on the data, another sensitivity analysis was performed. This time, the LE shape and blade edges positions were evaluated as the major parameters, with sweep-back angle playing an important role, too.

### 3.7 Final version

The final variant was estimated from the sensitivity analysis trends. The main goal was optimizing the inducer performance in 30% to 100% Q<sub>OPT</sub> range. While general recommendations for inducers are well known, data obtained by computations allowed

for more precise understanding of the trade-offs. Thanks to this, it was easier to tune the inducer for lower  $Q_s$  while maintaining its  $Q_{OPT}$  performance.

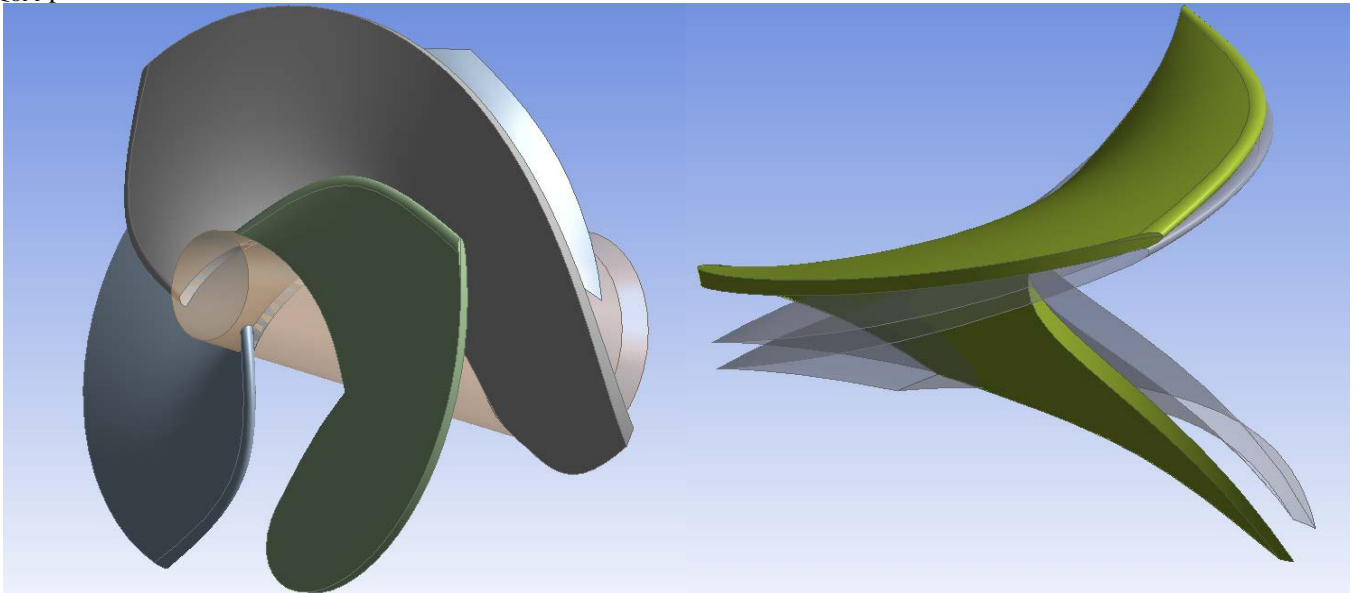


**Fig. 9** Inducer geometry and optimized blade (green) comparison with initial version (grey)

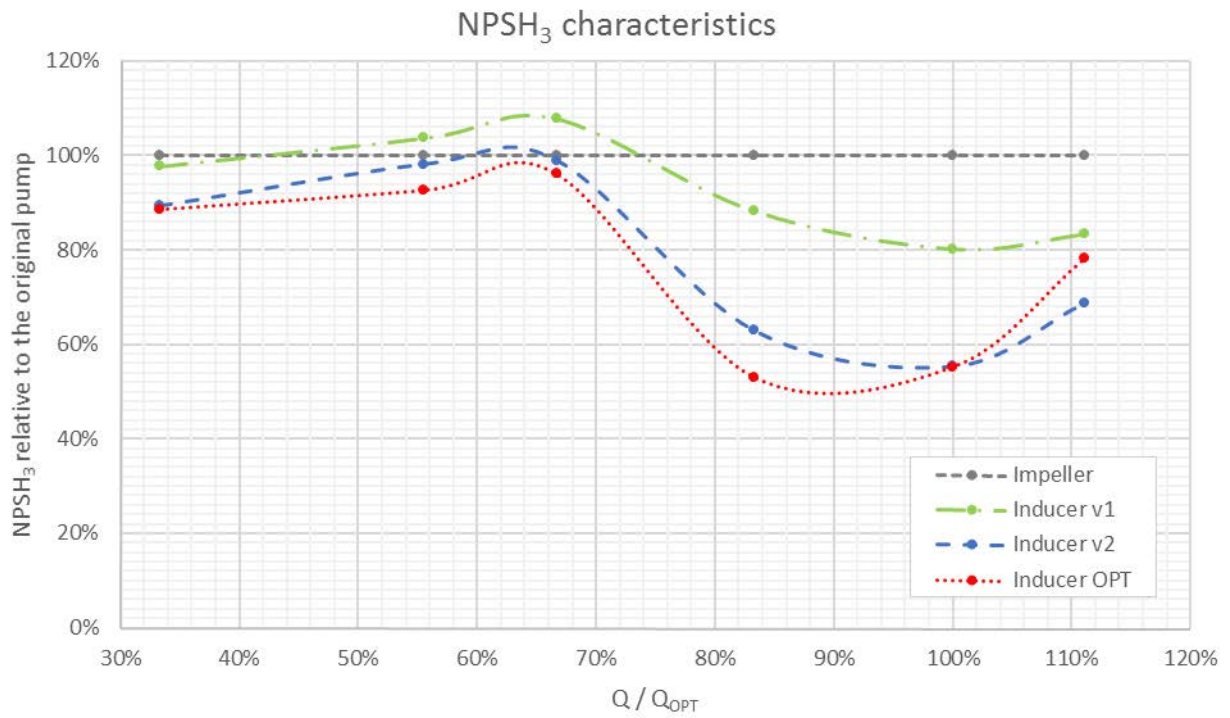


**Fig. 10** NPSH<sub>3</sub> comparison

The optimized variant shows an advantage from 40% to 90% of  $Q_{OPT}$ , without losing performance at the borders of the working range. The difference can also easily be observed in the cavitation areas (Figure 11).

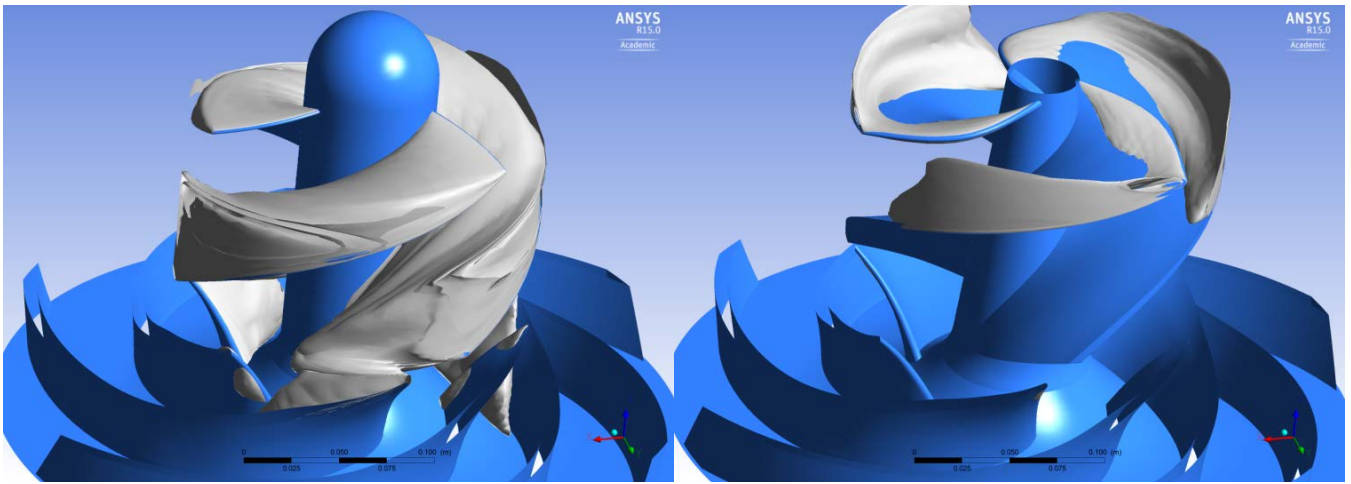


**Fig. 11** Cavitation areas in inducer and impeller for  $Q = 83\% Q_{OPT}$ . Original (left) and optimized (right) inducer.

Unfortunately, the results from the hydraulic laboratory and comparison to an experiment were not available at the time of writing the article. For showing the grid dependency of the results, one head drop curve computation with a refined mesh was performed.

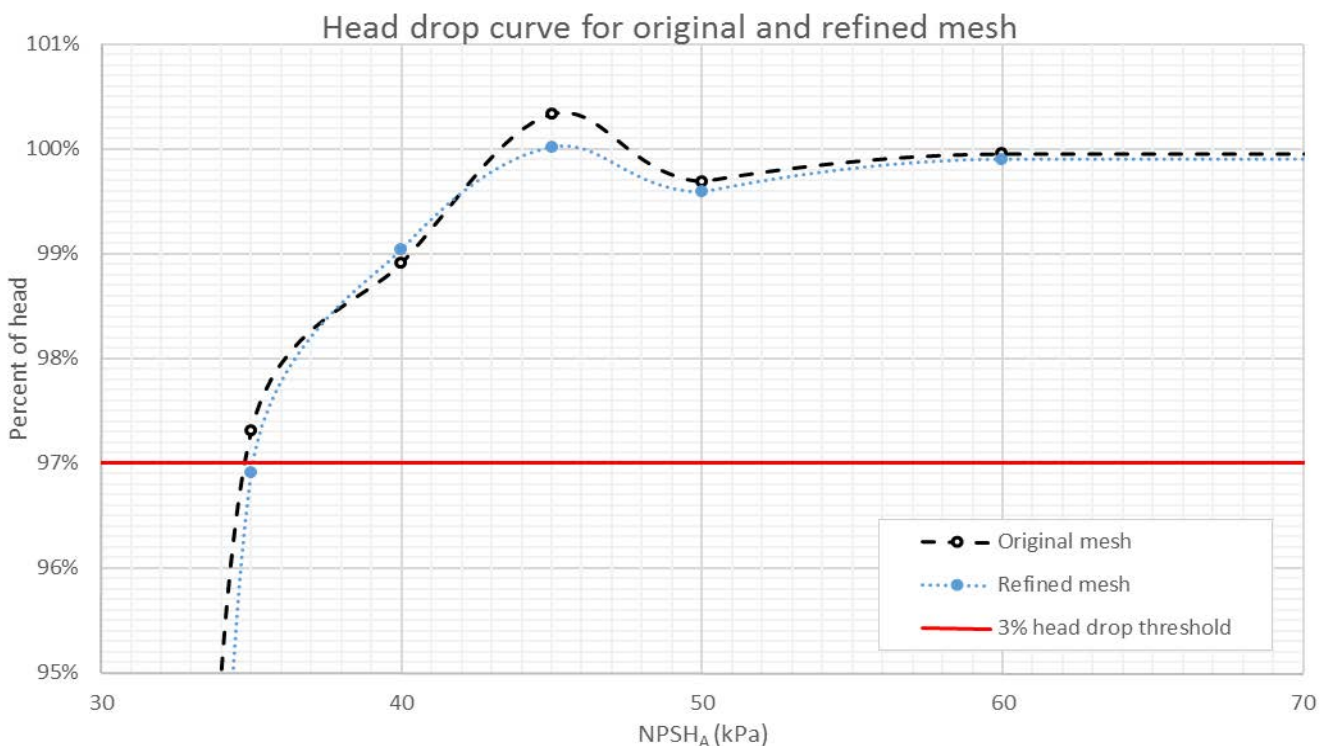


**Fig. 12** Head drop curves for the original and refined mesh.  $Q = 83\% Q_{OPT}$

For optimizing the resources usage, the refinement was mostly in the cavitation areas in the inducer and respected the flow direction. The number of nodes was 3.5 million, compared to 1.3 million for the original mesh. The whole  $NPSH_3$  was not computed due to the extreme computational demands. Doing so would require more resources than the whole previous optimization process. However, our experiences with many other pumps show this method of computing  $NPSH_3$  is reliable and in a good agreement with experimental data [6, 9].

#### 4. Conclusion

The combination of response surface and simplified TBR simulations was successfully employed for improving an inducer design. When compared to “traditional” method of computational cavitation performance evaluation, the total resources spent were similar to 5 to 10 design iterations. While hydraulic expertise and careful choice of design parameters and their evaluation still remains the crucial part of the design process, the numerical optimization is undoubtedly becoming an increasingly important part of it.

The future plans include adding an optimization algorithm to the final part of the process, using the sensitivity analysis estimated optimum as starting point. Another possibility is optimization based on a single-phase CFD analysis and pressure profile along the inducer blades. In literature [1] recommendations for fitting pressure distributions can be found.

Unfortunately, cavitation analysis still remains a very challenging numerical discipline. Especially due to the fact, that the cavitation areas alter passage shape and the fluid flow. This make different simplification generally unreliable, and fully-transient multiphase solution is required in many cases. Running and evaluating such simulations is very difficult, and the same is consequently true for shape optimization taking cavitation effects into account. Most probably, further development in computing



power will be crucial for this type of hydraulic design.

## 5. Acknowledgements

The work was performed with support of TA ČR project TE02000232 Special Rotary Machines Engineering Centre.

Computational resources were provided by the MetaCentrum under the program LM2010005 and the CERIT-SC under the program Centre CERIT Scientific Cloud, part of the Operational Program Research and Development for Innovations, Reg. no. CZ.1.05/3.2.00/08.0144.

## Nomenclature

$Q$	Flow rate	$Q_{OPT}$	Optimal flow rate
$NPSH$	Net Positive Suction Head [m]	$NPSH_3$	NPSH for which a 3% reduction in pump total head occurs [m]

## References

- [1] Sung, K., Young-Seok, Ch., Kyoung-Yong, L., Jun-Ho, K., 2011, "Design Optimization of Mixed-flow Pump in a Fixed Meridional Shape," International Journal of Fluid Machinery and Systems, Vol. 4, Issue 1, pp. 14-24.
- [2] Kim, S., Choi, Y. S., Lee, K. Y., Yoon, J. Y., 2009, "Design Optimization of Centrifugal Pump Impellers in a Fixed Meridional Geometry using DOE," International Journal of Fluid Machinery and Systems, Vol. 2, No. 2 pp. 172-178.
- [3] Tao, R., Xiao, R., Yang, W., Wang, F., Liu, W., "Optimization for Cavitation Inception Performance of Pump-Turbine in Pump Mode Based on Genetic Algorithm," Mathematical Problems in Engineering, Volume 2014 (2014), Article ID 234615
- [4] Kim, J.-H., Kim, K.-Y., "Optimization of Vane Diffuser in a Mixed-Flow Pump for High Efficiency Design," International Journal of Fluid Machinery and Systems, Vol. 4, No. 1, pp. 172-178.
- [5] Xie, S. F., Wang, Y., Liu, Z. C., Zhu, Z. T., Ning, C., Zhao, L. F., 2008, "Optimization of centrifugal pump cavitation performance based on CFD," IOP Conference Series: Materials Science and Engineering, Volume 72, Forum 3 - Pump Cavitation.
- [6] Sedlar, M., Sputa, O., Komarek, M., "CFD Analysis of Cavitation Phenomena in Mixed-Flow Pump," International Journal of Fluid Machinery and Systems, Vol. 5, No. 1, pp. 18-29.
- [7] Song, P., Zhang, Y., Xu, C., Zhou, X., Zhang, J., "Numerical studies on cavitation behavior in impeller of centrifugal pump with different blade profiles," International Journal of Fluid Machinery and Systems, Vol. 8, No. 2, pp. 94-101.
- [8] Zavadil, L., Kratky, T., Doubrava, V., 2014, "AXIAL DIFFUSER DEVELOPMENT USING ANSYS SOFTWARE TOOLS," Proceedings of 22nd SVS FEM ANSYS Users' Group Meeting and Conference, pp. 165-172.
- [9] Kratky, T., Sedlar, M., Bartonek, L., 2014, "FAST NPSH3 ANALYSIS USING TBR AND BATCH PROCESSING," Proceedings of 21st SVS FEM ANSYS Users' Group Meeting and Conference, pp. 110-117.
- [10] Gülich, J. H., 2008, Centrifugal Pumps Second Edition, Springer-Verlag Berlin Heidelberg